ASIAN JOURNAL OF CIVIL ENGINEERING (BHRC) VOL. 16, NO. 3 (2015)
PAGES 451-470

NURBS-BASED ANALYSIS OF CURVED ELEMENTS FOR THIN-WALLED STRUCTURES

H.R. Atri and S. Shojaee*
Department of Civil Engineering, Shahid Bahonar University of Kerman, Kerman, Iran

Received: 2 September 2014; **Accepted:** 20 December 2014

ABSTRACT

In the present investigation, static analysis of thin-walled shell-like structures based on isogeometric approach is presented. Since the higher order NURBS is well suited for describing the exact geometry and providing C^1-continuity, so they are used as basis functions for bridging the gap between design and analysis. The IGA method has been shown that the properties of the NURBS basis functions lead in many cases to superior accuracy per degree of freedom with respect to finite element method. So several thin shell structures are investigated by two approaches of rotation free thin shell element based on Kirchhoff theory and three dimensional solid element by using higher order NURBS basis functions through *k*-refinement strategy. It is observed that, 3D solid elements have no difficulties in dealing with curved edges and have good performance in modelling and analysis. For low order of NURBS basis functions, one can observe weak convergence rate, whereas for higher values of order of NURBS, the results are identical to those of shell element, which confirms that, only by applying the lengthwise of mesh refinement, the 3D solid element can have acceptable performance.

Keywords: IGA; NURBS; rotation free; solid element; shell.

1. INTRODUCTION

In a study of the mechanical behavior, two classifications of solid bodies are evident: first, bulky bodies which undergo imperceptible changes of shape, such as thick walls of a pressure vessel; second, thin bodies which are often quite flexible, such as the skin of an aircraft. However, localized behavior of a small element is similar in most bodies, and consequently, certain fundamentals apply to both categories.

The term solid is used to mean a three dimensional solid that is unrestricted as to shape, loading, material properties and boundary conditions. A consequence of this generality is

*E-mail address of the corresponding author: saeed.shojaee@uk.ac.ir (S. Shojaee)

that all six possible stresses (three normal and three shear) must be taken into account. Also, the displacement field involves all three possible components, u, v, and w. Problems of beam bending, plane stress, plates and shells can all be regarded as special cases of a 3D solid.

Shells, because of their distinct physical attributes (thinness and form) exhibit distinctly different behaviors. Shell structures are ubiquitous in nature and technology, so studying the behavior of these structures are of great importance and essential in predicting their structural responses. Different analytical approaches have been introduced for analysis of shells. Although the analytical methods are able to provide deep physical insights and their solutions are accurate, their application is often restricted to problems having simple geometries and boundary conditions. In practical cases, solutions based on numerical approaches are necessary and of course one of the most powerful methods for solving the complicated boundary and geometry problems is the finite element method (FEM), see [1]. Application of the finite element method for the analysis of solid and shell structures requires that the user have an understanding of the approximations involved in the development of elements and of course, before analyzing a structure using a shell element, one should always consider the direct application of three dimensional solids to model the structure. In many practical finite element methods, some portions of the structure are best modelled with shell elements and others with solids, for example, consider the case of a three dimensional arch dam. The arch dam may be thin enough to use shell elements to model arch section with six degrees of freedom per node; however modelling the foundation requires the use of solid element. Note that use of solid elements should be restricted to problem and analysis stages, such as verification, where the generality and flexibility of the full 3D model is warranted. On the other hand, in the finite element method, elements with curved surfaces can be used in the modelling. In finite element formulation of these types of elements, the mapping technique is the same with what used for other linear 3D solid elements [2]. As shown in Figure 1 in the physical coordinate system, elements with curved edges are first formed in the problem domain and then, these elements are mapped into the natural coordinate system, as can be seen, the element mapped in the natural coordinate system will have straight edges. In the finite element method, higher order elements of curved surfaces are often used for modelling curved boundaries, elements with excessively curved edged may cause problems in the numerical integration. Therefore more elements should be used where the curvature of the boundary is large. In addition, it is recommended that in the internal portion of the domain, an element with straight edges should be used whenever possible [2]. Although three dimensional finite elements offer more variety, it has many inherent disadvantages including, for instance, the cumbersome task of mesh generation; a high order, i.e. C^1-consistency, is not an easy task to construct conventionally conformable elements; locking phenomena which are mostly attributed to the use of low order basis functions and many different methods have been developed to prevent or reduce locking effects [3-12]; a time-consuming procedure for the connectivity of elements; remeshing in moving boundary problems and so on. Recently as an alternative to the FEM, a family of the so-called meshless or meshfree methods, e.g. see [13-17] have introduced to overcome the drawbacks of FEM. Some information on development of the meshless methods in solid mechanics can be found in Chen et al. [18].

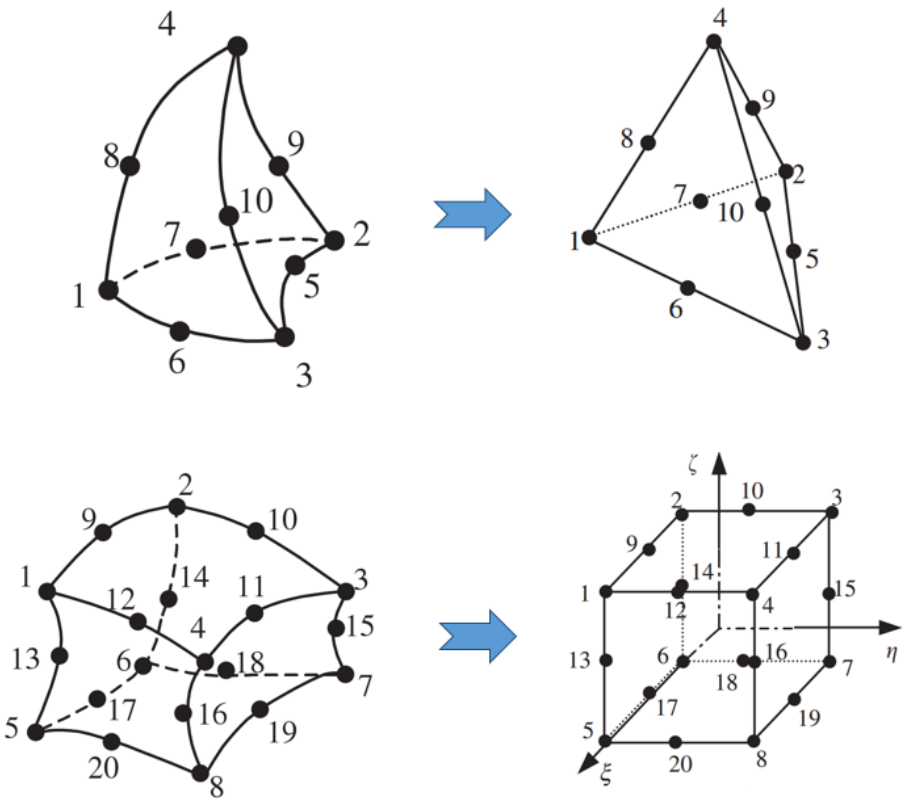

Figure 1. 3D elements with curved edges; physical coordinate system (left), natural coordinate system (right) [2]

The isogeometric analysis (IGA) proposed by Hughes et al. [19] and formalized more recently in the book of Cottrell et ali. [20] has been increasingly and successfully used in many engineering problems and has led to the publication of many works over the last nine years (see, for instance, [21-35]). This method offers the possibility of integrating finite element analysis (FEA) into conventional NURBS-based Computer Aided Design (CAD) tools. The IGA method handles many great features shared by both the FEM and the meshless methods. The basic idea behind IGA is to utilize the basic functions that are able to model accurately the exact geometries from the CAD point of view for numerical simulations of physical phenomena. It can be achieved by using the B-splines or NURBS for the geometrical description and invoke the isoparametric concepts to define the unknown field variables. A distinct advantage over the FEM is that mesh refinement is simply accomplished by re-indexing the parametric space without interaction with the CAD system. An intriguing trait of these functions is that they are typically smooth beyond the classical C^1-continuity of the standard FEM. The IGA-based approaches have been constantly developed and have shown many great advantages of research areas such as fluid-structure interaction [36-38], fracture mechanics [39], shells [40], structural vibration [41] and so on.

This paper presents a NURBS-based isogeometric approach for analysis of three dimensional structures with two viewpoints of shell and solid elements. NURBS-based analysis provides advantages especially for shells, since the structural behavior of a shell is

mainly determined by its geometry and therefore a good geometric description is essential. Furthermore, due to the exact geometry description with NURBS, curvatures can be evaluated directly on the surface without rotational degrees of freedom or nodal directions. So the displacement field is all three possible components in both elements, and by owing to higher order NURBS basis functions the curved edges in solid elements can be easily modeled and analyzed which shows the capability of NURBS basis functions in modelling the complex geometries and exact representation of common engineering shapes such as circles, cylinders. Spheres, and ellipsoids. Different benchmark examples are illustrated to show accuracy and convergence rate of shell element versus solid element which leads better understanding of their behaviors.

This paper is arranged as follow. Next section describes a brief review of NURBS basis functions. Section 3 presents the isogeometric formulation of solid and rotation-free thin shell elements. Section 4 gives numerical examples before the paper closes with concluding remarks.

2. B-SPLINES AND NURBS

NURBS are standard tools in Computer-Aided Design and computer graphics. In this section, a short description of isogeometric concepts is briefly presented. We shall not review the details of the concepts here, but refer the reader who is unfamiliar with the IGA to the references which are cited in this section.

2.1 B-splines

A B-spline is a non-interpolating, piecewise polynomial curve. It is defined by a set of control points, $\mathbf{P}_i$ (i=1,…,n) and a knot vector $\Xi=\{\xi_1,\xi_2,...,\xi_{n+p+1}\}$ where p is the polynomial degree of the curve and n is the number of basis functions corresponding to control points. The knot vector is a non-decreasing sequence of parametric coordinates ξ_i represent points in the parametric space of the curve. B-spline basis functions are defined recursively using Cox-de Boor formula [32]

$$N_{i,0}(\xi)=\begin{cases}1 & \text{if } \xi_i \le \xi \le \xi_{i+1}\\ 0 & \text{otherwise}\end{cases} \tag{1}$$

and for $p \ge 1$:

$$N_{i,p}(\xi)=\frac{\xi-\xi_i}{\xi_{i+p}-\xi_i}N_{i,p-1}(\xi)+\frac{\xi_{i+p+1}-\xi}{\xi_{i+p+1}-\xi_{i+1}}N_{i+1,p-1}(\xi) \tag{2}$$

Figure 2 shows an example of C^0 - continuity basis functions with an open knot vector. $\mathrm{H}=\{0, 0, 0, 0.2, 0.2, 0.4, 0.4, 0.6, 0.8, 1, 1, 1\}$.

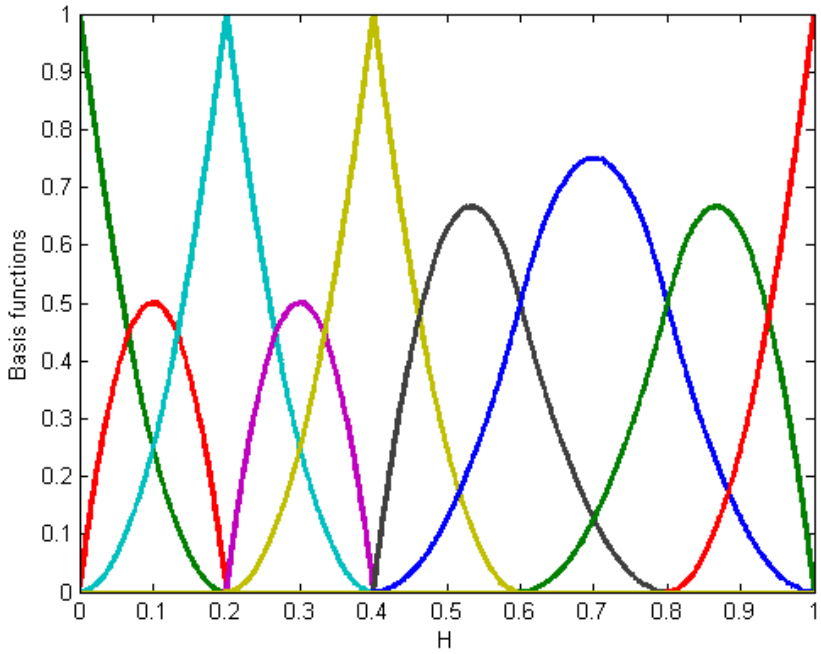

Figure 2. Non-uniform rational B-splines

2.1.1 B-splines curves

B-spline curve of degree p is computed by linear combination of control points and the respective basis functions:

$$\mathbf{C}(\xi) = \sum_{i=1}^{n} N_{i,p}(\xi)\mathbf{P}_i \tag{3}$$

2.1.2 B-splines surfaces

A B-spline surface is computed by the tensor product of B-spline basis functions in two parametric dimensions ξ and η , it is defined by a net of $n \times m$ control points, two knot vector Ξ and H, two polynomial degrees p and q (not necessary to be equal), and correspondingly basis functions $N_{i,p}(\xi)$ and $M_{j,q}(\eta)$ described as

$$\mathbf{S}(\xi,\eta) = \sum_{i=1}^{n}\sum_{j=1}^{m} N_{i,p}(\xi)M_{j,q}(\eta)\mathbf{P}_{i,j} \tag{4}$$

2.1.3 B-splines solids

B-splines solids are obtained analogously to B-splines surfaces, by considering a three dimensional net of control points $\mathbf{P}_{i\,j\,k}$, with $0 \le i \le n$, $0 \le j \le m$ and $0 \le k \le l$, where $N_{i,p}(\xi)$, $M_{j,q}(\eta)$ and $L_{k,r}(\zeta)$ are B-splines basis functions of degree p , q and r ,

respectively and the knot vectors Ξ, H and Z are specified as expressed previously:

$$\mathbf{S}(\xi,\eta,\zeta)=\sum_{i=1}^{n}\sum_{j=1}^{m}\sum_{k=1}^{l} N_{i,p}(\xi)M_{j,q}(\eta)L_{k,r}(\zeta)\mathbf{P}_{i,j,k} \tag{5}$$

2.2 NURBS

For a NURBS curve, each control point has an individual weight w_i, such a point $\mathbf{P}_i(x_i,y_i,z_i,w_i)$ can be represented with homogeneous coordinates $\mathbf{P}_i(w_i x_i,w_i y_i,w_i z_i,w_i)$ in a projective $\square^4$ space. Similarly to B-spline curves, surfaces and solids, NURBS-based ones are defined as [32]

$$\mathbf{C}(\xi)=\sum_{i=1}^{n} R_i^p(\xi)\mathbf{P}_i \tag{6a}$$

$$R_i^p(\xi)=\frac{N_{i,p}(\xi)w_i}{\sum_{\hat{i}=1}^{n} N_{\hat{i},p}(\xi)w_{\hat{i}}} \tag{6b}$$

$$\mathbf{S}(\xi,\eta)=\sum_{i=1}^{n}\sum_{j=1}^{m} R_{i,j}^{p,q}(\xi,\eta)\mathbf{P}_{i,j} \tag{7a}$$

$$R_{i,j}^{p,q}(\xi,\eta)=\frac{N_{i,p}(\xi)M_{j,q}(\eta)w_{i,j}}{\sum_{\hat{i}=1}^{n}\sum_{\hat{j}=1}^{m} N_{\hat{i},p}(\xi)M_{\hat{j},q}(\eta)w_{\hat{i},\hat{j}}} \tag{7b}$$

$$\mathbf{S}(\xi,\eta,\zeta)=\sum_{i=1}^{n}\sum_{j=1}^{m}\sum_{k=1}^{r} R_{i,j,k}^{p,q,r}(\xi,\eta,\zeta)\mathbf{P}_{i,j,k} \tag{8a}$$

$$R_{i,j,k}^{p,q,r}(\xi,\eta,\zeta)=\frac{N_{i,p}(\xi)M_{j,q}(\eta)L_{k,r}(\zeta)w_{i,j,k}}{\sum_{\hat{i}=1}^{n}\sum_{\hat{j}=1}^{m}\sum_{\hat{k}=1}^{r} N_{\hat{i},p}(\xi)M_{\hat{j},q}(\eta)L_{\hat{k},r}(\zeta)w_{\hat{i},\hat{j},\hat{k}}} \tag{8b}$$

Note that the weights play an important role in defining the basis, and if the weights are all equal, then $R_i^p(\xi)=N_{i,p}(\xi)$ and the curve is again polynomial. Thus B-splines are a special case of NURBS. In this work, only open knot vectors with at least of degree 2 in both spatial directions will be considered in the construction of NURBS entities. The mesh refinement, to be applied only lengthwise, will be of the *k*-refinement type, which means that C^{p-1}-continuity of the NURBS functions at knot spans is preserved. The positions of the control points and the values of the associated weights can be determined such as to build the geometry of the structure exactly. For a good review of mesh generation and refinement, see Cottrell et al. [20, Chapter 2].

Two examples of the geometry representation of a free-form shapes based on NURBS functions for a solid and surface are illustrated in Figure 3.

3. ISOGEOMETRIC FORMULATION BASED ON NURBS BASIS FUNCTIONS

Here, the application of NURBS-based isogeometric analysis is considered to formulate 2D

stress analysis problem and can be generalized to other problems. In isogeometric approach, the discretization is based on NURBS. Hence, the geometry and solution field are approximated as

$$x(\xi,\eta)=\sum_{k=1}^{n\times m}R_k \mathrm{P}_k \tag{9a}$$

$$u(\xi,\eta)=\sum_{k=1}^{n\times m}R_k d_k \tag{9b}$$

where $\xi,\eta\in\Omega_{patch}$ and $\Omega_{patch}=\left\{(\xi,\eta)\,|\,\xi\in\left[\xi_1,\xi_{n+p+1}\right],\eta\in\left[\eta_1,\eta_{m+q+1}\right]\right\}$. The matrix-form of $R_{i,j}$ and $P_{i,j}$ can be changed into vector-form by mapping from i,j subscripts to k by

$$k=i+(j-1)n \qquad \text{with} \qquad k=1,2,\ldots n\times m \tag{10}$$

The values of solution field at the control points, also called control variables, are displacements and can be arranged in a vector-form as follow

$$d_k=\{u_k,v_k,w_k\} \tag{11}$$

As can be seen, the displacement field is three possible components. In the following, the fundamental concepts of shell and solid elements are considered.

3.1 Kirchhoff-Love shell formulation

The finite element formulation based on the Kirchhoff theory requires elements with at least C^1-inter-element continuity, which has gained many difficulties to achieve for free form geometries when using the standard Lagrangian polynomials as basis functions. Higher-order NURBS basis functions, however, with an increased inter-element continuity can be easily obtained, thus the NURBS is well suited for the Kirchhoff elements by means of the IGA. In this paper, we have adopted the thin shell formulation from [40, 42].

In the Kirchhoff-Love shell theory, shell cross section remains normal to its mid-surface in the deformed configuration, which implies that the strain is assumed to be linear through the thickness and the transverse shear strains are zero. So the shell kinematics can be reduced to description of its mid-surface. For more details of thin shell formulation, see [43]. The configuration space of the generic shell $\boldsymbol{C}_s$ is defined as [44]:

$$\boldsymbol{C}_s = \left\{ \phi\left(\boldsymbol{R}, \boldsymbol{N}\right) : \mathrm{A} \to \mathbb{R}^3 \times \mathrm{S}^2 \right\} \tag{12}$$

Where A is the current surface of a shell, S is the space of admissible configuration, ϕ is the configuration or deformation and $\mathbb{R}$ is a set of real numbers, $\boldsymbol{N}\left(\xi_1, \xi_2\right) : \mathrm{A} \to \mathrm{S}^2$ is a unit vector associated with the middle surface of the shell and $\boldsymbol{R}\left(\xi_1, \xi_2\right) : \mathrm{A} \to \mathbb{R}^3$ specifies the position vector to each point on the shell's midsurface. The shell mid-surface is parameterized by curve linear coordinates ξ_1, ξ_2, ξ_3. The deformed shell geometry can be described by

$$\boldsymbol{x}\left(\xi_1, \xi_2\right) = \boldsymbol{X}\left(\xi_1, \xi_2\right) + \boldsymbol{u}\left(\xi_1, \xi_2\right) \tag{13}$$

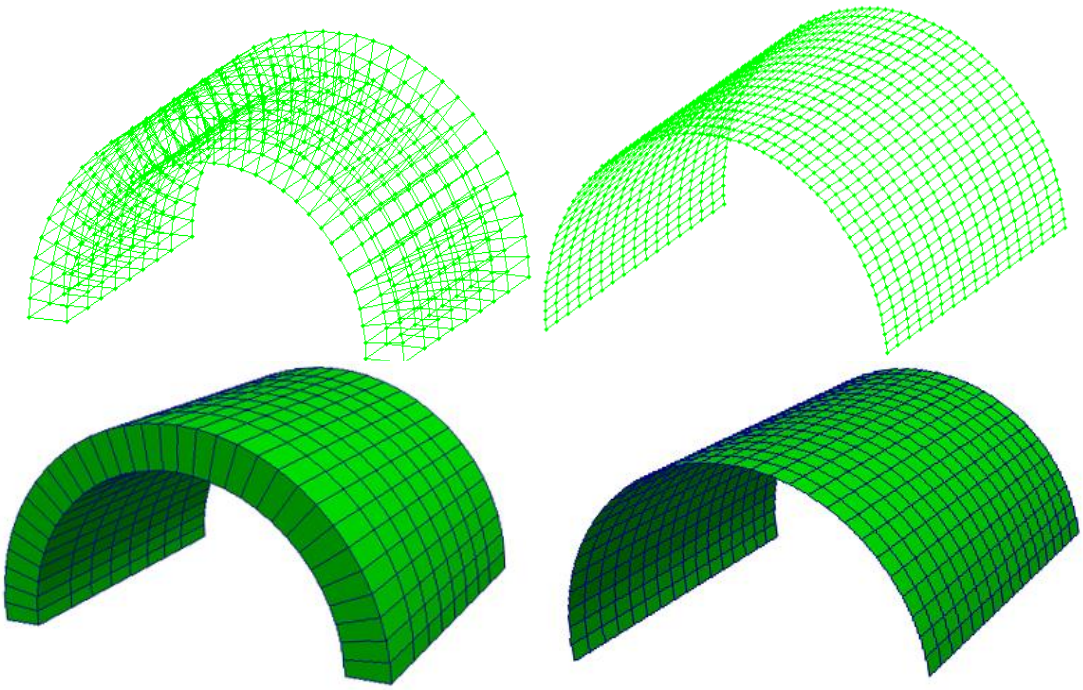

Figure 3. Physical mesh of an arch, solid NURBS (left), surface NURBS (right)

where $\boldsymbol{X}$ is the position vector of a material point of the shell mid-surface in the reference configuration, and $\boldsymbol{x}$ is the position vector of the same point in the deformed geometry. The shell geometry in the reference configuration is given by

$$\boldsymbol{X}\left(\xi_1, \xi_2, \xi_3\right) = \boldsymbol{R}\left(\xi_1, \xi_2\right) + \xi_3 \boldsymbol{N}_3 \qquad -\frac{h}{2} \le \xi_3 \le \frac{h}{2} \tag{14}$$

where $\boldsymbol{R}(\xi_1,\xi_2)$ specifies the position vector to each point on the shell's mid-surface, $\boldsymbol{N}_3$ is the normal to the mid-surface which can be obtained as $\boldsymbol{N}_3=\frac{\boldsymbol{N}_1\times\boldsymbol{N}_2}{\|\boldsymbol{N}_1\times\boldsymbol{N}_2\|}$, h represents the shell thickness and ξ_3 denotes the through the thickness coordinate. $\boldsymbol{N}_1$ and $\boldsymbol{N}_2$ are the basis vectors in the reference configuration which are given by

$$\boldsymbol{N}=\boldsymbol{R}_{,\alpha} \tag{15}$$

The Greek symbols take value of 1 and 2, and (,) indicates the partial derivative and similar for the shell geometry in the deformed configuration

$$\boldsymbol{x}(\xi_1,\xi_2,\xi_3)=\boldsymbol{r}(\xi_1,\xi_2)+\xi_3\boldsymbol{n}_3 \qquad -\frac{h}{2}\le\xi_3\le\frac{h}{2} \tag{16}$$

The uppercase quantities belong to the reference configuration, while lowercase ones denote to deformed configuration. The covariant basis vectors of the shell are

$$\boldsymbol{G}_\alpha=\frac{\partial\boldsymbol{X}}{\partial\xi_\alpha}=\boldsymbol{N}_\alpha+\xi_3\boldsymbol{N}_{3,\alpha} \qquad \boldsymbol{G}_3=\boldsymbol{N}_3 \tag{17}$$

$$\boldsymbol{g}_\alpha=\frac{\partial\boldsymbol{x}}{\partial\xi_\alpha}=\boldsymbol{n}_\alpha+\xi_3\boldsymbol{n}_{3,\alpha} \qquad \boldsymbol{g}_3=\boldsymbol{n}_3 \tag{18}$$

The covariant components of the metric tensor of the shell are given by

$$\mathrm{G}_{ij}=\boldsymbol{G}_i\cdot\boldsymbol{G}_j \tag{19}$$

$$g_{ij}=\boldsymbol{g}_i\cdot\boldsymbol{g}_j \tag{20}$$

i and j symbols range from 1 to 3. By the means of the well-known formula, the strain is

$$\boldsymbol{E}=E_{ij}\boldsymbol{G}^i\times\boldsymbol{G}^j \tag{14}$$

with

$$E_{ij}=\varepsilon_{ij}+\xi_3\varphi_{ij} \tag{15}$$

where $\boldsymbol{G}^i$ and $\boldsymbol{G}^j$ are the contravariant basis vectors, ε and φ which are membrane and bending strains, respectively can express as

$$\varepsilon_{ij} = \frac{1}{2}\left(\boldsymbol{n}_i \cdot \boldsymbol{n}_j - \boldsymbol{N}_i \cdot \boldsymbol{N}_j\right) \tag{16}$$

$$\varphi_{ij} = \boldsymbol{n}_i \cdot \boldsymbol{n}_{3,j} - \boldsymbol{N}_i \cdot \boldsymbol{N}_{3,j} \tag{17}$$

with the aid of Eq. **Error! Reference source not found.**, the strains for small deformations can be rewritten as

$$\varepsilon_{\alpha\beta} = \frac{1}{2}\left(\boldsymbol{G}_\alpha \cdot \boldsymbol{u}_{,\beta} - \boldsymbol{G}_\alpha \cdot \boldsymbol{u}_{,\alpha}\right) \tag{18}$$

$$\begin{aligned}\varphi_{\alpha\beta} = &-\boldsymbol{u}_{,\alpha\beta} + \frac{1}{\sqrt{\bar{j}}}\left[\boldsymbol{u}_{,1}\cdot\left(\boldsymbol{G}_{\alpha,\beta}\times\boldsymbol{G}_2\right) + \boldsymbol{u}_{,2}\cdot\left(\boldsymbol{G}_1\times\boldsymbol{G}_{\alpha,\beta}\right)\right] \\ &+ \frac{\boldsymbol{G}_3\cdot\boldsymbol{G}_{\alpha,\beta}}{\sqrt{\bar{j}}}\left[\boldsymbol{u}_{,1}\cdot\left(\boldsymbol{G}_2\times\boldsymbol{G}_3\right) + \boldsymbol{u}_{,2}\cdot\left(\boldsymbol{G}_3\times\boldsymbol{G}_1\right)\right]\end{aligned} \tag{19}$$

where $\bar{j} = \left\|\boldsymbol{g}_1 \times \boldsymbol{g}_2\right\|$.

In order to obtain the stiffness matrix, the internal virtual work is applied [40]

$$\begin{aligned}\delta \boldsymbol{W}_{\text{int}} &= \int_\Omega (\delta \boldsymbol{\varepsilon}^T \, \mathrm{D}_\mathrm{m} \, \boldsymbol{\varepsilon} + \delta \boldsymbol{\varphi}^T \, \mathrm{D}_\mathrm{b} \, \boldsymbol{\varphi}) \, d\Omega \\ &= \delta \boldsymbol{u}_I^T \int_\Omega [\,(\boldsymbol{B}_I^\mathrm{m})^T \, \mathrm{D}_\mathrm{m} \, \boldsymbol{B}_J^\mathrm{m} + (\boldsymbol{B}_I^\mathrm{b})^T \, \mathrm{D}_\mathrm{b} \, \boldsymbol{B}_J^\mathrm{b}\,] \, d\Omega \;\; \boldsymbol{u}_J\end{aligned} \tag{20}$$

where D_m and D_b are the membrane and bending constitutive matrix [43]. The internal stiffness matrix is obtained by

$$\mathbf{K} = \int_\Omega [\,(\boldsymbol{B}_e^\mathrm{m})^T \, \mathrm{D}_\mathrm{m} \, \boldsymbol{B}_e^\mathrm{m} + (\boldsymbol{B}_e^\mathrm{b})^T \, \mathrm{D}_\mathrm{b} \, \boldsymbol{B}_e^\mathrm{b}\,] \, d\Omega \tag{21}$$

where $\boldsymbol{B}_e^\mathrm{m}$ and $\boldsymbol{B}_e^\mathrm{b}$ are membrane and bending strain-displacement matrices, which can be derived according to Eq. (18) and Eq. (19).

3.2 Solid element formulation

A three dimensional solid element can be considered to be the most general of all solid finite elements, because all field variables are dependent of x**,** y and z. A 3D solid element can also have any arbitrary shape, material properties and boundary conditions in space. One of the major difficulties associated with the use of three dimensional elements is that, a large

number of elements have to be used for obtaining reasonably accurate results. This will result in a very large number of simultaneous equations to be solved in static analysis. Despite this difficulty, we may not have any other choice, except to use three dimensional elements in certain situations. So, in the following, a brief review of 3D solid element formulation is presented. More details regarding standard 3D elasticity can be found in the books of Belytschko et ali. [45] and Hughes [46].

By assuming the variations of the displacements in between the nodes to be linear, the displacements can be expressed by the interpolation functions used to describe the geometry as

$$\boldsymbol{U}(x,y,z) = \boldsymbol{R}(x,y,z)\cdot \boldsymbol{d}_e \tag{22}$$

where the nodal displacement vector, $\boldsymbol{d}_e$, is given as

$$\boldsymbol{d}_e = \begin{Bmatrix} u_1 \\ v_1 \\ w_1 \\ u_2 \\ v_2 \\ w_2 \\ u_3 \\ v_3 \\ w_3 \\ u_4 \\ v_4 \\ w_4 \\ \vdots \end{Bmatrix}_e \begin{matrix} \left.\begin{matrix} \\ \\ \end{matrix}\right\} \textit{displacement at control point 1} \\ \left.\begin{matrix} \\ \\ \end{matrix}\right\} \textit{displacement at control point 2} \\ \left.\begin{matrix} \\ \\ \end{matrix}\right\} \textit{displacement at control point 3} \\ \left.\begin{matrix} \\ \\ \end{matrix}\right\} \textit{displacement at control point 4} \end{matrix} \tag{23}$$

and the matrix of shape functions has the form

$$\boldsymbol{R} = \begin{bmatrix} R_1 & 0 & 0 & R_2 & 0 & 0 & R_3 & 0 & 0 & R_4 & 0 & 0 & \dots \\ 0 & R_1 & 0 & 0 & R_2 & 0 & 0 & R_3 & 0 & 0 & R_4 & 0 & \dots \\ 0 & 0 & R_1 & 0 & 0 & R_2 & 0 & 0 & R_3 & 0 & 0 & R_4 & \dots \end{bmatrix} \tag{24}$$

$$\underbrace{\qquad}_{ControlPoint\ 1} \quad \underbrace{\qquad}_{ControlPoint\ 2} \quad \underbrace{\qquad}_{ControlPoint\ 3} \quad \underbrace{\qquad}_{ControlPoint\ 4}$$

which $\boldsymbol{R}$ is the NURBS basis functions. Stress-strain relations are written in the form

$$\begin{Bmatrix} \sigma_x \\ \sigma_y \\ \sigma_z \\ \tau_{xy} \\ \tau_{yz} \\ \tau_{zx} \end{Bmatrix} = \begin{bmatrix} (1-\upsilon)\cdot\boldsymbol{c} & \upsilon\cdot\boldsymbol{c} & \upsilon\cdot\boldsymbol{c} & 0 & 0 & 0 \\ \upsilon\cdot\boldsymbol{c} & (1-\upsilon)\cdot\boldsymbol{c} & \upsilon\cdot\boldsymbol{c} & 0 & 0 & 0 \\ \upsilon\cdot\boldsymbol{c} & \upsilon\cdot\boldsymbol{c} & (1-\upsilon)\cdot\boldsymbol{c} & 0 & 0 & 0 \\ 0 & 0 & 0 & G & 0 & 0 \\ 0 & 0 & 0 & 0 & G & 0 \\ 0 & 0 & 0 & 0 & 0 & G \end{bmatrix} \cdot \begin{Bmatrix} \varepsilon_x \\ \varepsilon_y \\ \varepsilon_z \\ \gamma_{xy} \\ \gamma_{yz} \\ \gamma_{zx} \end{Bmatrix} \tag{25}$$

where $\boldsymbol{c} = \dfrac{E}{(1+\nu)\cdot(1-2\nu)}$ and $G = \dfrac{E}{2(1+\nu)}$ (E and ν are the Young's modulus and Poisson's ratio, respectively). Or the compact form is $\{\sigma\} = [\boldsymbol{E}]\cdot\{\varepsilon\}$.

The strain-displacement relations are:

$$\begin{aligned} \varepsilon_x &= \frac{\delta u}{\delta x} & \varepsilon_y &= \frac{\delta v}{\delta y} & \varepsilon_z &= \frac{\delta w}{\delta z} \\ \gamma_{xy} &= \frac{\delta u}{\delta y} + \frac{\delta v}{\delta x} & \gamma_{yz} &= \frac{\delta v}{\delta z} + \frac{\delta w}{\delta y} & \gamma_{xz} &= \frac{\delta u}{\delta z} + \frac{\delta w}{\delta x} \end{aligned} \tag{26}$$

and if we group all the strain components in a vector, we can write $\{\varepsilon\} = [\boldsymbol{B}]\cdot\{\boldsymbol{U}\}$. Once the strain matrix has been obtained, the stiffness matrix $\boldsymbol{K}$ for 3D solid elements can be obtained as

$$\boldsymbol{K} = \int_V [\boldsymbol{B}]^T \cdot [\boldsymbol{E}]\cdot[\boldsymbol{B}]\, dV \tag{27}$$

In the present study, sufficiently accurate Gaussian quadrature is utilized on knot spans and the numerical results are obtained using $(p+1)(q+1)$ Gauss points in shell element and $(p+1)(q+1)(r+1)$ in solid element, which p, q and r are the orders of NURBS basis functions. So far, the isogeometric analysis has been shown to be more accurate than traditional finite element per degree of freedom. As NURBS are rational polynomials, Gaussian quadrature seems to be very effective for integrating them.

4. NUMERICAL RESULTS

In this section, the validity and the accuracy of the isogeometric approach in thin-walled shell-like structures are investigated. The examples are modelled by three dimensional solid elements and Kirchhoff shell elements with no rotational degree of freedom. The results obtained by isogeometric analysis are also compared with analytical solutions.

4.1 Scordelis-Lo roof

Scordelis-Lo roof shown in Figure 4 is a panel of a cylindrical shell that is supported at its ends by rigid diaphragms, inhibiting the x and z translations. The roof is subjected to a uniform gravity load. The vertical displacement at the midpoint of the side edge is given as the reference solution. Geometric, material data and boundary conditions of the problem are shown in Figure 4. Due to symmetry, only a quadrant of the roof is discretized and the results are shown in Figure 5 and Figure 6 for different polynomial orders and reference solution. As it can be seen, by increasing the order of NURBS in 3D solid element, the convergence rate appears satisfactory, it should be noted that, *k*-refinement strategy is used and there are only 2 elements through the thickness. And in shell element, for all polynomial orders, the convergence rate is fast.

The analytical solution of the mid-side vertical displacement, (Point B) is normally taken as 0.3024 [47, 48], even though, a value of 0.3086 was originally presented by Scordelis and Lo [49]. Figure 7 shows the deflection at the midpoint of the free edge for quadrant of

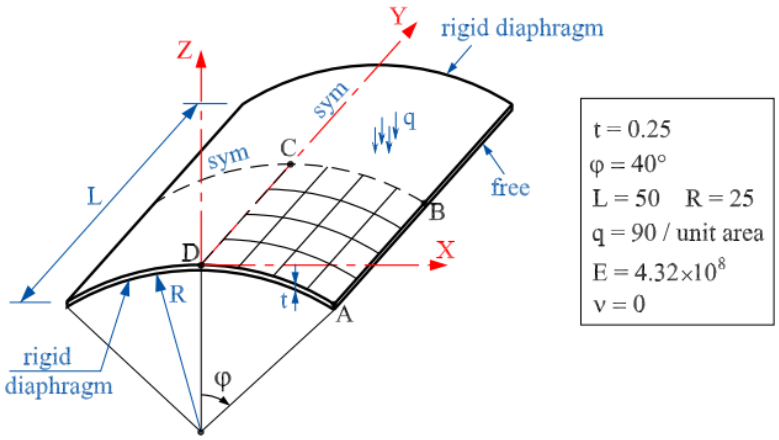

Figure 4. Scordelis-Lo roof, geometry and material data [50]

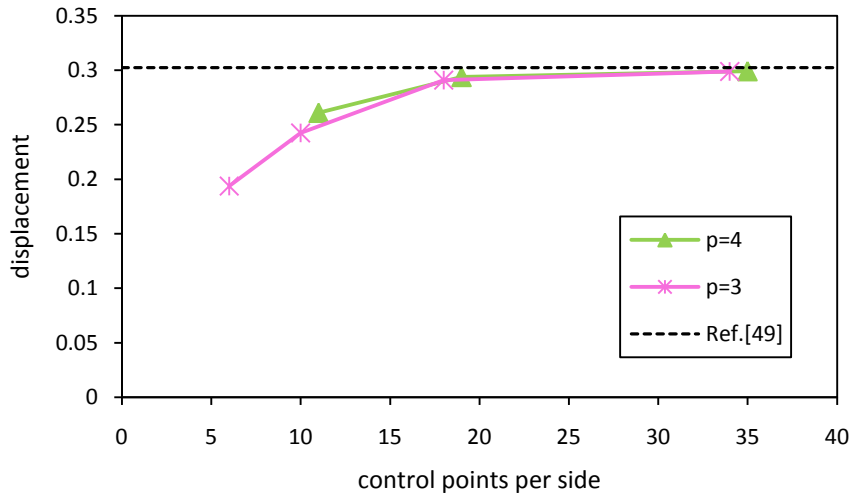

Figure 5. Scordelis-Lo roof; vertical displacement at the midpoint of free edge, (solid element)

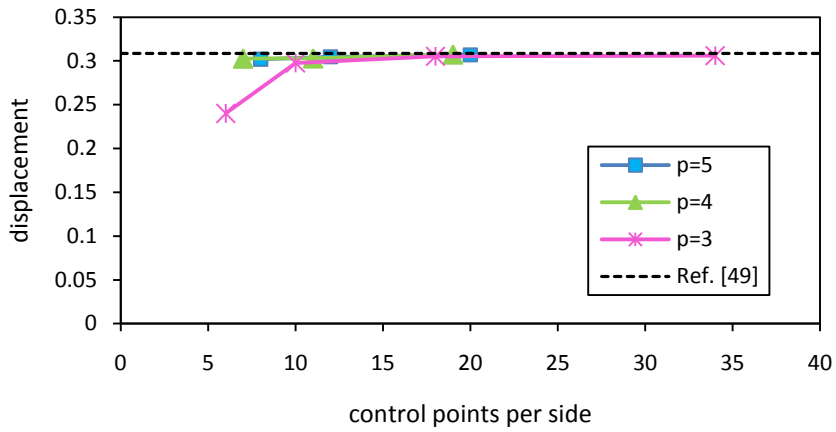

Figure 6. Scordelis-Lo roof; vertical displacement at the midpoint of free edge, (shell element)

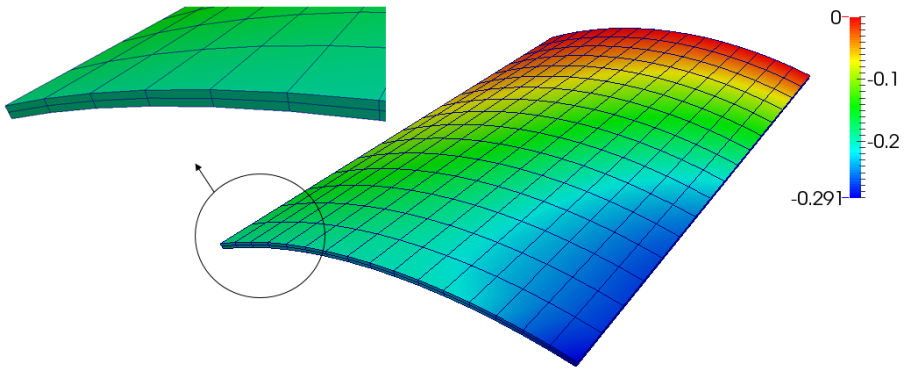

Figure 7. Quadrant of Scordelis-Lo roof, deformed configuration, (solid element)

Scordelis-Lo roof, and the physical mesh for the roof by solid element is depicted in Figure 8. Finally, the deformed configuration for the entire roof using shell element is shown in Figure 9.

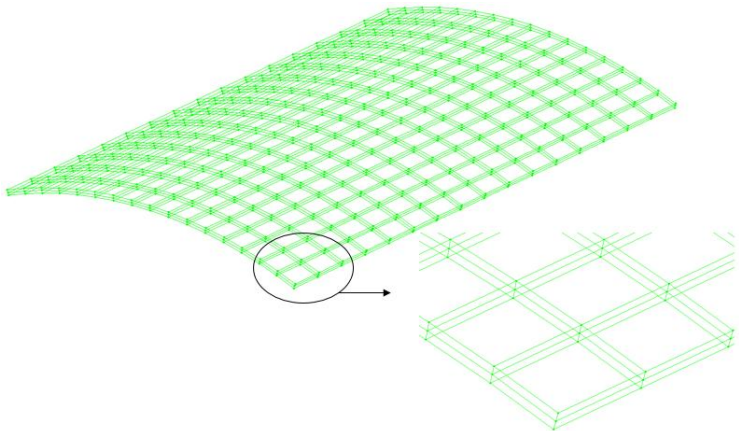

Figure 8. Quadrant of Scordelis-Lo roof, physical mesh, (solid element)

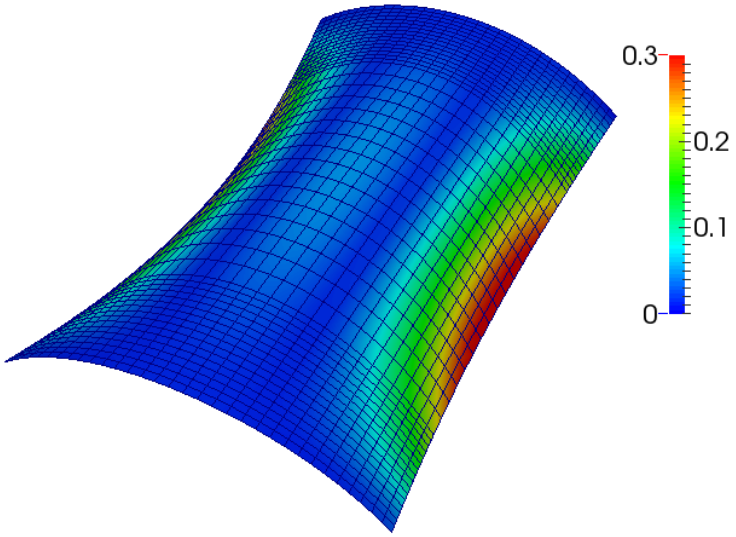

Figure 9. Scordelis-Lo roof, deformed configuration, (shell element)

4.2 Pinched cylinder with diaphragms

The pinched cylinder with diaphragms is one of the most severe tests for both inextensional bending modes and complex membrane states. The cylinder is subjected to two opposite point loads in the middle. The geometrical and material properties of the cylinder are depicted in Figure 10. Taking advantage of symmetry, only one eighth of the geometry is modelled.

The theoretical solution of deflection at the loading point is 1.8248×10^{-5} [47]. Figure 11-12 show numerical results for the radial displacement at the loading point for both elements. It is observed that, the performance of the shell element is in excellent agreement with the analytical solution for different order of NURBS basis functions. It is interesting to point out that the solid element faces difficulties converging at low order of NURBS basis functions, but with increasing the order of NURBS, the convergence rate is similar to the shell element, which shows that, by lengthwise refinement as like as shell element, and only with 2 elements through the thickness, the 3D solid element can have satisfactory performance. In the following, the deformed configuration and the physical mesh for one octant of pinched cylinder by solid element is shown in Fig. Figure 13-14, respectively.

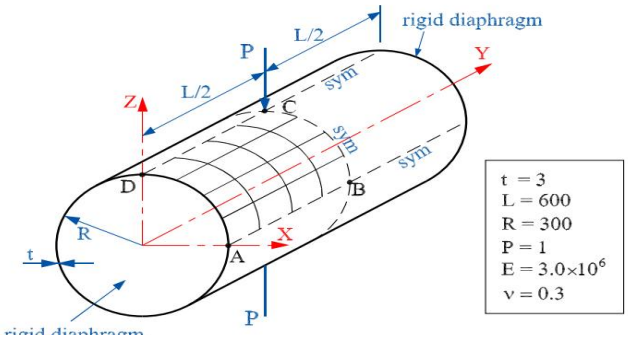

Figure 10. Pinched cylinder, geometry and material data [50]

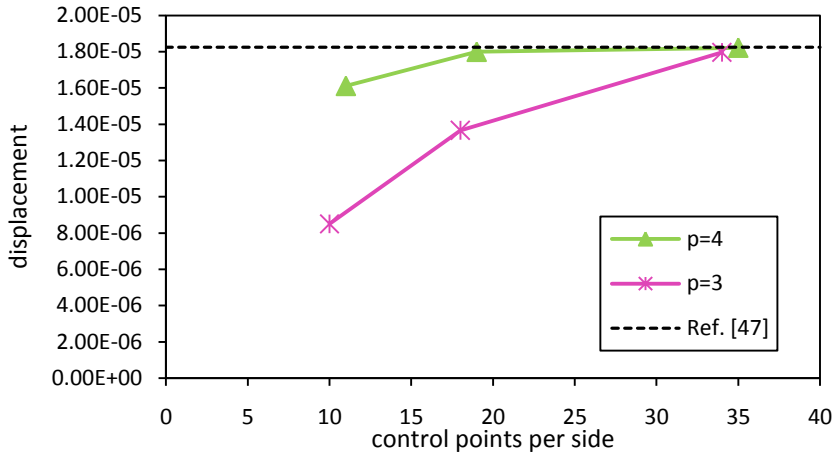

Figure 11. Pinched cylinder; radial displacement at the loading point, (solid element)

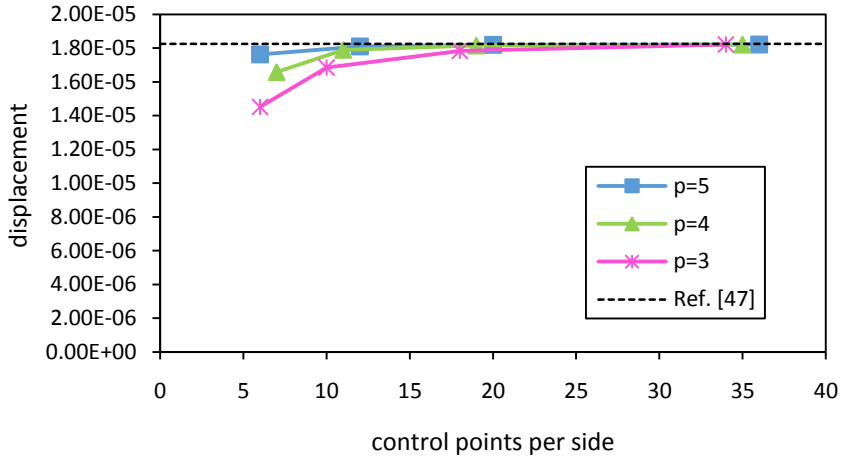

Figure 12. Pinched cylinder; radial displacement at the loading point, (shell element)

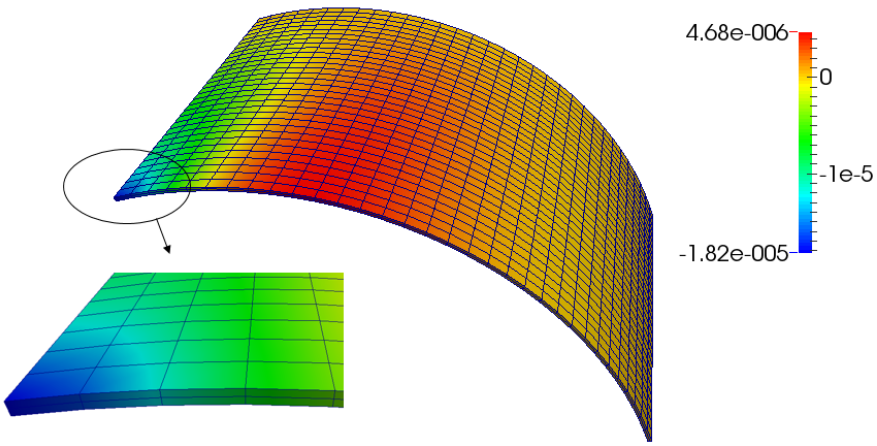

Figure 13. One octant of pinched cylinder, deformed configuration, (solid element)

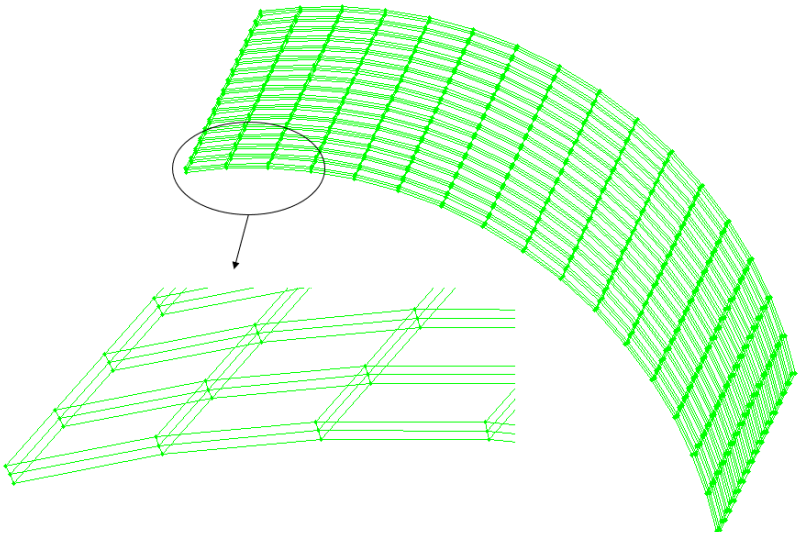

Figure 14. One octant of pinched cylinder, physical mesh, (solid element)

5. CONCLUSION

In this paper, NURBS-based isogeometric analysis is applied to study static analysis of thin-walled shell-like structures. The analysis has been carried out using higher order NURBS basis functions. With NURBS, achieving the C^1-continuity of Kirchhoff-Love shell theory can be provided easily. The number of degrees of freedom are lower because only the middle surface of a rotation-free thin shell is modelled, and by owing to higher order NURBS basis functions, the curved edges in solid elements can be easily modelled and analyzed. From the detailed numerical study, it can be seen that the 3D solid element in isogeometric analysis, in contrast to finite element method, has no difficulties in dealing with curved surfaces, and its performance is found to be better when using higher order NURBS basis functions. It is interesting to note that 3D solid element appears to converge monotonically to the reference solution and its convergence rate indeed appears satisfactory.

REFERENCES

1. Zienkiewicz OC, Taylor RL, Zhu JZ. *The Finite Element Method, Its Basis and Fundamentals*, Elsevier, 6th edition, Oxford, 2005.
2. Liu GR, Quek SS. *The Finite Element Method: A Practical Course*, Butterworth-Heinemann, 1st edition, Oxford, 2003.
3. Gellert M. A new method for derivation of locking-free plate bending finite via mixed/hybrid formulation, *International Journal for Numerical Methods in Engineering*, **26**(1988) 1185-1200.
4. Kabir HRH. A shear locking free isoparametric three-node triangular finite element for moderately thick and thin plates, *International Journal for Numerical Methods in Engineering*, **35**(1992) 503-19.

5. Bletzinger KU, Bischoff M, Ramm E. A unified approach for shear-locking free triangular and rectangular shell finite elements, *Computers and Structures*, **75**(2000) 321-34.
6. Cesar de Sa JMA, Natal Jorge RM, Fontes Valente RA, Almeida Areias PM. Development of shear locking-free shell elements using an enhanced assumed strain formulation, *International Journal for Numerical Methods in Engineering*, **53**(2002) 1721-50.
7. Braess D. Enhanced assumed strain elements and locking in membrane problems, *Computer Methods in Applied Mechanics and Engineering*, **165**(1998) 155-74**.**
8. Yunhua L. Explanation and elimination of shear locking and membrane locking with field consistence approach, *Computer Methods in Applied Mechanics and Engineering*, **162**(1998) 249-69**.**
9. Babuska I, Suri M. Locking effects in the finite element approximation of elasticity problems, *Numerische Mathematik*, **62**(1992) 439-63.
10. Arnold DN, Brezzi F. Locking-free finite element methods for shells, *Mathematics of Computations*, **66**(1997) 1-14.
11. Stolarski H, Belytschko T. Membrane locking and reduced integration for curved elements, *Journal of Applied Mechanics*, **49**(1982) 172-6.
12. Babuska I, Suri M. On locking and robustness in the finite element method, *SIAM Journal of Numerical Analysis*, **29**(1992) 1261-93.
13. Belytschko T, Lu YY, Gu L. Element free Galerkin method, *International Journal for Numerical Methods in Engineering*, **37**(1994) 229-56.
14. Liu WK, Jun S, Zhang YF. Reproducing kernel particle method, *International for Numerical Methods in Fluids*, **20**(1995) 1081-1106.
15. Atluri SN, Zhu T. A new meshless Petrov-Galerkin (MLPG) approach, *Computational Mechanics*, **22**(1998) 117-27.
16. Liu GR, Gu YT. A point interpolation method for two dimensional solids, *International Journal for Numerical Methods in Engineering*, **50**(2001) 937-51.
17. Bui QT, Nguyen NM, Zhang Ch. An efficient meshfree method for vibration analysis of laminated composite plates, *Computational Mechanics*, **48**(2011) 175-93.
18. Chen Y, Lee JD, Eskandarian A. *Meshless Methods in Solid Mechanics*, Springer, 4th edition, 2006.
19. Hughes TJR, Cottrell JA, Bazilevs Y. Isogeometric analysis: CAD, finite elements, NURBS, exact geometry and mesh refinement, *Computer Methods in Applied Mechanics and Engineering*, **194**(2005) 4135-95**.**
20. Cottrell JA, Hughes TJR, Bazilevs Y. *Isogeometric Analysis: Toward Integration of CAD and FEA*, Wiley, Chichester, 2009.
21. Cottrell JA, Hughes TJR, Reali A. Studies of refinement and continuity in isogeometric structural in isogeometric structural analysis, *Computer Methods in Applied Mechanics and Engineering*, **196**(2006) 5257-96.
22. Hughes TJR, Reali A, Sangalli G. Duality and unified analysis of discrete approximations in structural dynamics and wave propagation: comparison of *p*-method finite elements with *k*-method NURBS, *Computer Methods in Applied Mechanics and Engineering*, **197**(2008) 4104-24.
23. Kiendl J, Bazilevs Y, Hsu MC, Wüchner R. and Bletzinger KU. The bending strip

method for isogeometric analysis of Kirchhoff–Love shell structures comprised of multiple patches, *Computer Methods in Applied Mechanics and Engineering*, **199**(2010) 2403-16.
24. Benson D, Bazilevs Y, Hsu MC, Hughes TJR. A large deformation, rotation-free, isogeometric shell, *Computer Methods in Applied Mechanics and Engineering*, **200**(2011) 1367-78.
25. Benson D, Bazilevs Y, Hsu MC, Hughes TJR. Isogeometric shell analysis: the Reissner-Mindlin shell, *Computer Methods in Applied Mechanics and Engineering*, **199**(2010) 276-89.
26. Echter R, Bischoff M. Numerical efficiency, locking and unlocking of NURBS finite elements, *Computer Methods in Applied Mechanics and Engineering*, **199**(2010) 374-82.
27. Elguedj T, Bazilevs Y, Calo VM, Hughes TJR. B-bar and F-bar projection methods for nearly incompressible linear and nonlinear elasticity and plasticity using higher order NURBS element, *Computer Methods in Applied Mechanics and Engineering*, **197**(2007) 5257-96.
28. Beiro da Veiga L, Buffa A, Lovadina C, Martinlli M, Sangalli G. An isogeometric method for Reissner-Mindlin plate bending problem, *Computer Methods in Applied Mechanics and Engineering*, **209**(2012) 45-53.
29. Beiro da Veiga L, Lovadina C, Reali A. Avoiding shear locking for the Timoshinko beam via isogeometric collocation methods, *Computer Methods in Applied Mechanics and Engineering*, **241**(2012) 38-51.
30. Thai CH, Nguyen-Xuan H, Nguyen-Thanh N, Le TH, Nguyen-Thoi T, Rabczuk T. Static, free vibration, and buckling analysis of laminated composite Reissner–Mindlin plates using NURBS-based isogeometric approach, *International Journal for Numerical Methods in Engineering*, **91**(2012) 571-603.
31. Bouclier R, Elguedj T, Combescure A. Locking free isogeometric formulations of curved thick beams, *Computer Methods in Applied Mechanics and Engineering*, **245**(2012) 144-62.
32. Piegl L, Tiller W. *The Nurbs Book*, Springer-Verlag, 2nd edition, New York, 1997.
33. Hughes TJR, Reali A, Sangalli G. Efficient quadrature for NURBS-based isogeometric analysis, *Computer Methods in Applied Mechanics and Engineering*, **199**(2010) 301-13.
34. Auricchio F, Calabro F, Hughes TJR, Reali A, Sangalli G. A simple algorithm for obtaining nearly optimal quadrature rules for NURBS-based isogeometric analysis, *Computer Methods in Applied Mechanics and Engineering*, **249**(2012) 15-27.
35. Jari H, Atri HR, Shojaee S. Nonlinear thermal analysis of functionally graded material plates using a NURBS based isogeometric approach, *Composite Structures*, **119**(2014) 333-45.
36. Bazilevs Y, Calo VM, Zhang Y, Hughes TJR. Isogeometric fluid–structure interaction analysis with applications to arterial blood flow, *Computational Mechanics*, **38**(2006) 310-22.
37. Bazilevs Y, Calo VM, Hughes TJR, Zhang Y. Isogeometric fluid-structure interaction: theory, algorithms, and computations, *Computational Mechanics*, **43**(2008) 3-37.
38. Zhang Y, Bazilevs Y, Goswami S, Bajaj C, Hughes TJR. Patient-specific vascular NURBS modeling for isogeometric analysis of blood flow, *Computer Methods in Applied Mechanics and Engineering*, **196**(2007) 2943-59.

39. Shojaee S, Asgharzadeh M, Haari A. Crack analysis in orthotropic media using combination of isogeometric analysis and extend finite element, *International Journal of Applied Mechanics,* doi: 10.1142/S1758825114500677.
40. Kiendl J, Bletzinger KU, Linhard J, Wüchner R. Isogeometric shell analysis with Kirchhoff–Love elements, *Computer Methods in Applied Mechanics and Engineering,* **198**(2009) 3902-14.
41. Cottrell JA, Reali A, Bazilevs Y, Hughes TJR. Isogeometric analysis of structural vibrations, *Computer Methods in Applied Mechanics and Engineering*, **195**(2006) 5257-96.
42. Nguyen-Thanh N, Kiendl J, Nguyen-Xuan H, Wüchner R, Bletzinger KU, Bazilevs Y, Rabczuk T. Rotation free isogeometric thin shell analysis using PHT-splines, *Computer Methods in Applied Mechanics and Engineering,* **200**(2011) 3410-24.
43. Bischoff M, Wall WA, Bletzinger KU, Ramm E. *Models and Finite Elements For Thin-Walled Structures*, Encyclopedia of Computational Mechanics, 2nd edition, 2004.
44. Simo JC, Fox DD. On a stress resultant geometrically exact shell model. Part I: Formulation and optimal parameterization, *Computer Methods in Applied Mechanics and Engineering*, **72**(1989) 267-304.
45. Belytschko T, Liu WK, Moran B. *Nonlinear Finite Elements For Continua and Structures*, John Wiley & Sons, New York, 2013.
46. Hughes TJR. *The Finite Element Method: Linear Static and Dynamic Finite Element Analysis*, Courier Dover Publications, Mineola, 2012.
47. MacNeal RH, Harder RL. A proposed standard test problems to test finite element accuracy. *Finite Element in Analysis and Design*, **1**(1985) 3-20.
48. Belytschko T, Stolarski H, Liu WK, Carpenter N, Ong JSJ. Stress projection for membrane and shear locking in shell finite elements, *Computer Methods in Applied Mechanics and Engineering*, **51**(1985) 221-58.
49. Scordelis AC, Lo KS. Computer analysis of cylindrical shells, *ACI Journal Proceedings*, **61**(1964) 539-62.
50. Nguyen-Van H, Mai-Duy N, Tran-Cong T. An improved quadrilateral flat element with drilling degrees of freedom for shell structural analysis, *CMES: Computer Modeling in Engineering and Sciences,* **49** (2009) 81-110.